Itinerant-electron magnetocrystalline anisotropy energy of YCo_5 and related compounds

Lutz Steinbeck,* Manuel Richter, and Helmut Eschrig
Department of Theoretical Solid State Physics, IFW Dresden e.V., P.O. Box 270016, D-01171 Dresden, Germany
(Received 13 September 2000; published 23 April 2001)

The contribution of the itinerant states to the magnetocrystalline anisotropy (MA) energy of YCo_5 and isostructural compounds has been calculated using a fully relativistic optimized LCAO band-structure scheme within the framework of density-functional theory in local spin density approximation (LSDA), and its dependence on lattice geometry and Fe substitution has been investigated. Additionally taking into account orbital polarization, a correction to LSDA accounting for Hund's second rule, enhances the calculated orbital moments, orbital moment anisotropies and MA energies, and leads to good agreement with available experimental data for YCo_5. The MA energies are found to be strongly affected by changes of the lattice geometry (c/a ratio and volume) resulting from (i) uniaxial strain in YCo_5 and (ii) the lanthanide contraction along the RCo_5 (R=Y, La, Pr, Nd, Sm, Gd) series, because of the sensitivity of the MA energy to changes of the band structure. We obtain a large variation of the MA energy of RCo_5 along the R series which is shown to be predominantly a lattice geometry effect. It is in contrast to the commonly assumed independence of the transition-metal sublattice MA on the R constituent. The calculated band-filling dependence of the MA energies of ordered $Y(Co_{1-x}Fe_x)_5$ compounds (x=0,0.4,0.6,1.0) qualitatively explains the experimentally observed concentration dependence of the MA energy in $Y(Co_{1-x}Fe_x)_5$ pseudobinaries at low Fe concentrations.

DOI: 10.1103/PhysRevB.63.184431 PACS number(s): 75.30.Gw, 71.20.Lp

I. INTRODUCTION

The intrinsic properties required from rare-earth (R) transition-metal (T) intermetallics, if they are to be suitable candidates for permanent magnet materials, are a high Curie temperature and saturation magnetization and a strong uniaxial magnetocrystalline anisotropy (MA). The MA energy, defined as the change of the ground-state energy of a magnet upon rotation of the magnetization direction with respect to the crystal axes, is a purely relativistic effect. In RT intermetallics, it arises from two major sources: (i) the spin-orbit (SO) interaction of the itinerant states (mainly the T $3d$ states) which couples the magnetization direction (mainly carried by the spin) to the anisotropic crystal environment and (ii) the interaction of the localized partially filled R $4f$ shell (with $4f$ spin and orbital moment practically rigidly coupled to each other by SO interaction) with the crystal field. Anisotropy contributions from other sources like magnetic dipolar interaction or anisotropic exchange are in general small by comparison, although they can be appreciable in some cases. Extrinsic (shape) anisotropy is not considered here.

At low temperatures, the $4f$ anisotropy usually exceeds the 3d contribution (except for rare earths with empty, half-filled or completely filled $4f$ shells which do not interact with the crystal field in first order), but because of the strong temperature dependence of the $4f$ anisotropy the two contributions can be of comparable size at room temperature. For example, the anisotropy constant K_1 of YCo_5, where no $4f$ anisotropy occurs, amounts to 7.4 MJ/m^3 at 4.2 K and 5.8 MJ/m^3 at room temperature.[1] The corresponding values for the permanent magnet compound $SmCo_5$ are 30 MJ/m^3 and 17 MJ/m^3, respectively.[2] Moreover, density-functional calculations[3] show that, in principle, even higher T anisotropies are possible in uniaxial T or RT systems.

The evaluation of the MA energy originating from itinerant states by means of electronic-structure calculations is a long-standing interesting but difficult problem.[4] Considerable progress has been made in recent years. Besides the elemental $3d$ ferromagnets,[5–8] $3d$ monolayers and multilayers,[9–11] $3d$-$4d$ and $3d$-$5d$ compounds and alloys,[12–15] and ferromagnetic actinide compounds[16] have been studied. For the class of RT intermetallics, results have been reported on YCo_5,[3,17–19] YFe_3Co_2 and YFe_5,[20] and $YFe_{11}Ti$.[21] Several techniques have been devised to deal with the computational problems arising from (i) the smallness of the anisotropy energies, which amount to between 1 and 1000 μeV/atom depending on the crystal structure and the strength of the spin-orbit coupling, in comparison with typical total energies of solids and (ii) the slow convergence of the required Brillouin zone (BZ) integrations. These problems are much more severe for cubic T systems, where the MA energy is of the order of 1 μeV/atom, than for the RT intermetallics, whose anisotropy energies are in general much larger because of their low crystal symmetry, but still the calculation of the MA energy remains a challenging task, since the MA energy may strongly depend on details of the band structure.

In view of the strong dependence of the itinerant-electron MA energy on band structure and band filling found in the calculations, it should be possible to modify the MA energy significantly by manipulating (i) the band filling by substitutions of the T atoms and (ii) the band structure either directly or indirectly (via lattice geometry effects) by substitutions, interstitial atoms, growth as thin film on suitably chosen substrates or by external pressure.

In the present work, we investigate the itinerant-electron MA energy for several RT intermetallics with hexagonal $CaCu_5$ structure. A prototypical compound is YCo_5 which exhibits a large MA and which has been particularly well studied experimentally[1,22–25] and theoretically.[3,17–20] First, we calculate the spin and orbital moments, orbital moment

anisotropies (OMA) and anisotropy energy of YCo_5 in order to compare them with results of previous studies. Going beyond the previous studies, we then analyze the dependence of these quantities on the lattice geometry, especially on the c/a ratio. The influence of substituting Fe for Co is investigated by performing calculations for YFe_5 and the ordered pseudobinaries YCo_3Fe_2 and YFe_3Co_2, with particular emphasis on the band-filling dependence of the MA energy, which is related to the composition dependence in a rigid-band picture. Furthermore, we compare the itinerant-electron MA energies of several RCo_5 (R=Y, La, Pr, Nd, Sm, Gd) compounds in order to check whether the MA energies of isostructural compounds with different rare earths are indeed more or less the same, an assumption which is frequently made when deriving the $4f$ anisotropy from magnetization measurements on RT intermetallics.[26] Finally, we decompose the calculated MA energies into site contributions in two different ways and discuss the suitability of such decompositions, which have also been made on the basis of experimental results, for predicting the MA energies of isostructural compounds.

The paper is organized as follows. After a brief outline of the MA of RT intermetallics (Sec. II) we describe our method (Sec. III) and present and discuss our results on YCo_5 and related compounds (Sec. IV). A brief summary with some conclusions is given in Sec. V.

II. MAGNETOCRYSTALLINE ANISOTROPY IN RARE-EARTH TRANSITION METAL INTERMETALLICS

The magnetic properties of RT intermetallics are usually described in terms of a two-sublattice model taking into account the effective exchange interactions within and between the R and T sublattices in a mean-field approximation and the interaction with the crystal field.[27–29] The interaction between T $3d$ and R $4f$ electrons is mediated by hybridization between transition-metal $3d$ and rare-earth $5d$ states and intraatomic local $5d$-$4f$ exchange.[30] In iron- and cobalt-rich RT intermetallics the TT exchange interaction is large compared to the RR interaction, whereas the RT interaction is in general intermediate between these two, but in most cases large enough to assume the R and T sublattices to be almost rigidly coupled by isotropic RT exchange proceeding via the R $5d$ states. So both sublattice magnetization vectors can only be rotated simultaneously, and the R and T anisotropy contributions can simply be added to give the total MA. Other sources of anisotropy like dipolar, exchange, or magnetoelastic interactions yield usually only small additional contributions to the MA. As an exception, the dipolar interaction is considered to be the main source of the difference between the magnetocrystalline anisotropies of isostructural Y-T and Gd-T intermetallics because of the large Gd $4f$ moments. This difference was found to be non-negligible in comparison with the T sublattice anisotropy in R_2Co_{17}.[31]

Due to the different nature of the strongly correlated localized $4f$ electrons and the itinerant $3d$ electrons their MA energy contributions require different approaches for calculation on a density-functional basis. The following hierarchy of interactions governs the behavior of the $4f$ electrons in the considered $3d$-$4f$ intermetallics:

$$U_{\mathrm{eff}}^{4f} \gg E_{\mathrm{so}}^{4f} \gg E_{\mathrm{ex}}^{4f\text{-}3d} \gg E_{\mathrm{cf}}^{4f}, \tag{1}$$

where U_{eff}^{4f} is the effective atomic Coulomb correlation energy, E_{so}^{4f} the spin-orbit coupling energy of the $4f$ electrons, $E_{\mathrm{ex}}^{4f\text{-}3d}$ the (indirect, via R $5d$ states) exchange interaction between the $3d$ and $4f$ electrons and E_{cf}^{4f} the interaction energy with the crystal field. As a consequence, the $4f$ anisotropy is of single-ion character and can be well described within the single-ion crystal-field model,[32–34] the starting point of which is the atomic limit. In this approach, the interaction of the $4f$ shell as a whole with the crystal field is treated within perturbation theory. The degeneracy of the J eigenstates with respect to J_z in the free atom is lifted in the crystal, leading to crystal-field splittings and inducing a MA. Since recently, the $4f$ crystal-field splittings and MA contributions can also be obtained from density-functional calculations, within the limits of the single-ion model, in reasonable agreement with experiment (see Ref. 29 for a survey).

The energy hierarchy corresponding to Eq. (1) for the T $3d$ electrons in $3d$-$4f$ intermetallics looks entirely different:

$$W^{3d} > U_{\mathrm{eff}}^{3d} > E_{\mathrm{ex}}^{3d-3d} > E_{\mathrm{ex}}^{3d-4f} \approx E_{\mathrm{cf}}^{3d} \gg E_{\mathrm{so}}^{3d}. \tag{2}$$

Since the effective $3d$ Coulomb correlation energy U_{eff}^{3d} is smaller than the bandwidth W^{3d} the $3d$ states have to be treated as band states. $E_{\mathrm{ex}}^{3de\text{-}3d}$ is the exchange interaction between the $3d$ electrons and $E_{\mathrm{ex}}^{3d\text{-}4f}$ the (indirect) exchange interaction with the R $4f$ electrons. E_{cf}^{3d} stands for the crystal-field splitting of the $3d$ states which determines the energy difference between the centers of gravity of the related bands. Because of the itinerant character of the $3d$ states in the compounds considered in this work, the anisotropy of their hybridization, i.e., the dependence of the band dispersion on the azimuthal quantum number, which is strong in uniaxial crystals, is more important for the MA than the crystal-field splitting.[35] Although the spin-orbit coupling is smallest here, a perturbative treatment would be very much complicated by the entanglement of **k** dependent degeneracies due to band crossings. For a calculation of the MA energy of the $3d$ states their spin-orbit coupling needs to be explicitly taken into account. This requires fully relativistic band structure calculations.

The atomic d shell total orbital angular momentum L is partially quenched by crystal field and hybridization in the solid but is in general still nonzero. In uniaxial crystals, the hybridization of the d orbitals depends strongly on their azimuthal quantum number and, consequently, the orbital moment acquires an anisotropy. The SO splitting will then be different for different orientations of the magnetization, and, thus, give rise to a total-energy difference, a MA energy. The changes will be particularly large if degeneracies are lifted for bands in the vicinity of the Fermi level. In a strong ferromagnet, the spin-down d band is at the Fermi level,

whereas the spin-up d band is almost filled and does, therefore, not contribute significantly to d orbital moment, OMA and MA energy.

Because of the close relationship between the MA energy and the OMA, an adequate description of the orbital moment is crucial for MA calculations. The orbital moments obtained from relativistic band structure calculations in the local-spin-density approximation (LSDA) are usually too small in comparison with experiment, because they are only induced by the spin polarization via spin-orbit coupling in this approximation. The orbital polarization effect described by Hund's second rule in atoms is still present to a certain degree in the solid. In order to account for this effect, Eriksson, Brooks, and Johansson[36] introduced an orbital polarization (OP) energy proportional to L^2 which is derived from atomic theory. It is assumed that this dependence transfers to the solid. This correction to LSDA yields enhanced orbital moments which are in better agreement with experiment for transition metals, actinides and intermetallic compounds.[37,38] Usually, the enhanced orbital moments lead to larger OMAs and MA energies, again improving agreement with experiment.

III. METHOD

The calculations reported in this work are based on density-functional theory in the LSDA using the Perdew-Zunger[39] parametrization of the Ceperley-Alder[40] exchange-correlation potential. We employ a self-consistent optimized linear combination of atomic orbitals (LCAO) method[41] in a scalar-relativistic and a fully relativistic[42] version. The $4f$ electrons are treated in the so-called open-core approximation which logically corresponds to LSDA+U with a large U. OP corrections were included for d states.

In the fully relativistic version, the single particle spinors are calculated as eigenstates of the squared Dirac operator $\Omega=(D^2-c^4)/2c^2$, projected on the electron sector, where D is the effective Kohn-Sham-Dirac operator and c the velocity of light. In contrast to the Dirac operator D, the operator Ω is bounded from below. This procedure facilitates a variational ansatz for the calculation of the atomic basis states. The effective four-component equation is solved without perturbation approaches.

The minimum valence basis consists of $5s$, $5p$, and $4d$ ($6s$, $6p$, and $5d$) states at the R site and $4s$, $4p$, and $3d$ states at the transition-metal sites. Core states are recalculated in the modified atomic site potential within each step of the self-consistency cycle. The valence states are orthogonalized to the core states. The Kohn-Sham potential is built up from overlapping extended spherical atomic site potentials, implying that nonspherical effects in the ''interstitial'' region are taken into account self-consistently. This approximation should be superior to the atomic sphere approximation (ASA) which has been employed for the calculations of itinerant-electron MA energies of RT intermetallics published so far.[3,17–21,43] We checked the accuracy of our calculated scalar-relativistic band structures, particularly in the vicinity of the Fermi energy, by comparing them to the scalar-relativistic band structures obtained with the more time-consuming full-potential local orbital (FPLO) scheme.[44]

The MA energy is the change of the ground-state energy upon rotation of the magnetization direction with respect to the crystal axes. So, in principle, it can be obtained from independent self-consistent relativistic total-energy calculations performed with two different orientations of the magnetization. However, the spin-orbit splitting of the valence states in RT intermetallics is much smaller than the exchange splitting and the band width (the spin-orbit parameters are approximately 80, 50, 40, and 100 meV for Co $3d$, Fe $3d$, Y $4d$, and Gd $5d$ states, respectively). Therefore, it is justified to first solve the Kohn-Sham equations for the scalar-relativistic Hamiltonian self-consistently and to include the spin-orbit coupling in a subsequent one-step calculation. The Kohn-Sham eigenvalues obtained in this last calculational step depend on the magnetization direction $\hat{\mathbf{n}}$. As a consequence of the force theorem,[45,5] the change in total energy upon inclusion of the spin-orbit coupling is given by the change in the single-particle eigenvalues to first order in the changes of electron and spin densities. Hence we obtain the MA energy as the difference of the sum of the valence electron energies between the two magnetization directions:

$$\Delta E=E(\hat{\mathbf{n}}_2)-E(\hat{\mathbf{n}}_1)=\sum_{n\mathbf{k}}^{\mathrm{occ.}(\hat{\mathbf{n}}_2)}\varepsilon_{n\mathbf{k}}(\hat{\mathbf{n}}_2)-\sum_{n\mathbf{k}}^{\mathrm{occ.}(\hat{\mathbf{n}}_1)}\varepsilon_{n\mathbf{k}}(\hat{\mathbf{n}}_1), \tag{3}$$

which includes a possible change of the Fermi energy by summing over all occupied states up to the respective Fermi levels $\varepsilon_F(\hat{\mathbf{n}}_1)$ and $\varepsilon_F(\hat{\mathbf{n}}_2)$. The force theorem has been shown[46] to yield MA energies in good agreement with those obtained from total-energy calculations for uniaxial systems and even for cubic systems, although doubts on the validity of the force theorem for the calculation of the MA energy in cubic systems have been raised,[47] based on the argument that the band energy difference is of the same (fourth) order in the spin-orbit splitting as the Hartree term.

In order to account for the intra-atomic Coulomb correlations (Hund's second rule), we include an OP energy quadratic in the orbital angular momentum L,[36] approximating the energy difference between the Hund's rule ground-state term and the weighted average of the terms with maximum S of an atomic d^n configuration. It is assumed that this dependence is transferred to the solid, where suitably site-projected crystal quantities replace the corresponding atomic quantities. The OP shifts the atomic single-electron eigenvalues or the diagonal elements of the crystal Hamiltonian, respectively, by

$$\Delta E_{l\sigma m_l}=-B_{l\sigma}L_\sigma m_l. \tag{4}$$

L_σ is the orbital moment of spin channel σ, m_l the azimuthal quantum number of the orbital in question and $B_{l\sigma}$ the Racah parameter which takes the form[3]

$$B_{d\sigma}=\frac{9F^2_{d\sigma}-5F^4_{d\sigma}}{441} \tag{5}$$

TABLE I. Racah parameters $B^{\uparrow}$ and $B^{\downarrow}$ for Co and Fe $3d$ and Y $4d$ spin-up and spin-down states, respectively, as obtained in the present calculation (in meV) for YCo_5 and YFe_5.

Site	$B^{\uparrow}$	$B^{\downarrow}$
Co($3g$)	148	143
Co($2c$)	147	143
Fe($3g$)	137	132
Fe($2c$)	137	131
Y($1a$)	77	77

for d states, with the Slater F^k integrals

$$F^k_{d\sigma}=\int dr_1\, r_1^2 \int dr_2\, r_2^2 \Phi^2_{d\sigma}(r_1)\Phi^2_{d\sigma}(r_2)\frac{r_<^k}{r_>^{k+1}} \qquad (6)$$

calculated from the radial d wave functions $\Phi_{d\sigma}$. Here, $r_<=\min(r_1,r_2)$ and $r_>=\max(r_1,r_2)$. The OP shift Eq. (4) derives from an OP energy of the form $-BL^2/2$ deduced from atomic theory as described above. We include this OP shift for the T $3d$ and Y $4d$ (R $5d$) states. The Racah parameters obtained in the present calculation for the crystallographically inequivalent sites in YT_5 (T=Fe,Co) are given in Table I. The OP shifts in the solid have to be determined self-consistently since the orbital moments and the OP shifts are interrelated by Eq. (4). Hence, in those calculations where the OP correction was included, we performed a self-consistent relativistic calculation with the magnetization parallel to the (0001) direction. This yields orbital moments L_σ and OP shifts for the m_l orbitals with respect to (0001) as quantization axis. The same shifts are then applied to m_l orbitals with respect to $(\bar{1}2\bar{1}0)$ as quantization axis in a one-step calculation where the magnetization was oriented along the $(\bar{1}2\bar{1}0)$ direction. A similar procedure has been used in other MA energy calculations where the force theorem was employed in connection with the OP correction.[3,18] In order to check the accuracy of this procedure, we performed another self-consistent relativistic calculation with OP correction where the magnetization was oriented parallel to the $(\bar{1}2\bar{1}0)$ direction; see Sec. IV B below.

The BZ integrations were done with the linear tetrahedron method. For the self-consistent band structure calculations we used 133 **k** points in the irreducible part (1/24) of the hexagonal BZ. No significant changes of the results were found by increasing this number to 407. Changing the magnetization direction from (0001) to $(\bar{1}2\bar{1}0)$ or $(10\bar{1}0)$ in the basal plane lowers the symmetry of the system to orthorhombic (with 1/8 of the BZ as irreducible part). In order to eliminate errors arising from nonequivalent **k** grids, we calculated the band sums with the lower-symmetry irreducible part and **k** grid for both magnetization directions. The convergence of the resulting MA energies with respect to the number of **k** points was checked carefully for all calculations reported in this work; cf. Sec. IV B.

YCo_5 crystallizes in the hexagonal $CaCu_5$ structure (Fig. 1), space group no. 191, D^1_{6h} ($P6/mmm$), with two inequivalent Wyckoff sites $2c$ and $3g$ for Co. It is a layered structure consisting of Y-Co layers interchanging with pure Co layers. The experimental lattice parameters[2,48–50] of the RCo_5 compounds which were used in the present work are given in Table II.

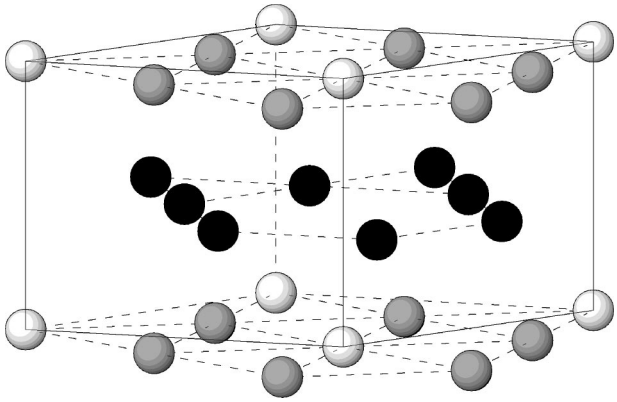

FIG. 1. Hexagonal $CaCu_5$ structure of RT_5 with R($1a$) (open symbols), T($2c$) (shaded symbols), and T($3g$) (filled symbols) sites.

IV. RESULTS AND DISCUSSION

A. Spin and orbital moments of YCo_5

The total magnetization, spin and orbital moments and their anisotropies of YCo_5 obtained from (a) a self-consistent scalar-relativistic calculation followed by one-step calculations including spin-orbit coupling (SO) for magnetization directions (0001) and $(\bar{1}2\bar{1}0)$, respectively, and (b) a self-consistent relativistic calculation (including SO coupling and OP correction) with the magnetization in the (0001) direction followed by a one-step relativistic calculation including spin-orbit coupling and orbital polarization correction (SO+OP) for the other magnetization direction, as described in the previous section, are given in Table III. Experimental data derived from spin-polarized neutron scattering,[24] single-crystal magnetization,[1] and hyperfine-field measurements[22] are also included for comparison.

Including the OP correction strongly enhances the orbital moments, while the spin moments are only marginally affected by relativistic self-consistency and orbital polarization. The Co spin moment is found to be slightly larger at the

TABLE II. Experimental lattice parameters a and c and c/a ratios of RCo_5 used for the present calculations.

	La[a]	Nd[b]	Sm[c]	Pr[b]	Gd[b]	Y[d]
a (Å)	5.1085	5.0055	5.004	5.0055	4.9632	4.928
c (Å)	3.9667	3.9775	3.969	3.9940	3.9670	3.992
c/a	0.7765	0.7946	0.7932	0.7979	0.7993	0.8101
V (Å^3)	89.649	86.305	86.069	86.663	84.628	83.958

[a]Reference 50.
[b]Reference 49.
[c]Reference 48.
[d]Reference 2.

TABLE III. Magnetization M, spin and orbital moments (in μ_B) and their anisotropies of YCo_5 obtained from calculation (a), including spin-orbit coupling only (SO), and (b), including both spin-orbit coupling and orbital polarization (SO+OP), respectively; see text. The upper values in each line of the table correspond to magnetization direction (0001). The anisotropies [between the $(\bar{1}\bar{2}10)$ and (0001) direction] are given by the lower value in each line of the table. The corresponding anisotropy energies ΔE are shown at the bottom of the table (in meV/f.u.). In the last two columns, experimental values obtained from spin-polarized neutron scattering (Ref. 24), magnetization (Ref. 1), and hyperfine field (Ref. 22) measurements are given for comparison.

	SO		SO+OP		Experiment	
	spin	orbital	spin	orbital	spin	orbital
Y($1a$)	-0.18	-0.03	-0.18	-0.01		
	0.015	-0.012	0.013	-0.020		
Co($3g$)	1.52	0.11	1.52	0.26	1.44[a]	0.28[a], 0.24[b]
	-0.002	-0.005	-0.002	-0.020		
Co($2c$)	1.46	0.13	1.47	0.33	1.31[a]	0.46[a], 0.26[b]
	-0.001	-0.018	-0.005	-0.053		
Total	7.30	0.57	7.32	1.41		
	0.008	-0.067	-0.003	-0.186		
M	7.87		8.73		8.3[c]	
	-0.06		-0.19		-0.3[c]	
ΔE	0.58		4.4		3.8[c]	

[a]Reference 24.
[b]Reference 22.
[c]Reference 1.

$3g$ site than at the $2c$ site, in agreement with the relative size of the spin moments derived from spin-polarized neutron diffraction studies of Schweizer and Tasset.[24] We obtain a higher Co orbital moment at the $2c$ site than at the $3g$ site. This is in accordance with the order of site orbital moments reported in Ref. 24 but the size of the orbital moments and their difference between the two Co sites are larger in experiment. In contrast to these neutron scattering data, the orbital moments derived from hyperfine-field measurements[22] differ only marginally between the two Co sites. From density-functional calculations, Daalderop *et al.*[3] and Yamaguchi and Asano[19,43] obtained almost identical orbital moments for the two Co sites whereas Nordström *et al.*[18] found the orbital moment to be larger at the $2c$ site.

Magnetization measurements on single crystals[1] revealed a large anisotropy of the magnetization between the c axis and the basal plane which reaches 4% of the total magnetization at 4.2 K. When including orbital polarization in the way described in Sec. III, we find a magnetization anisotropy of about 2% which almost exclusively originates from the orbital part of the magnetization. In comparison with the experimental data, the total magnetization is slightly overestimated by the calculation including orbital polarization, while the magnetization and its anisotropy are underestimated if only the spin-orbit coupling is included. A polarized neutron study on $NdCo_5$ (also included in Ref. 1) below and above the spin reorientation temperature range suggested that

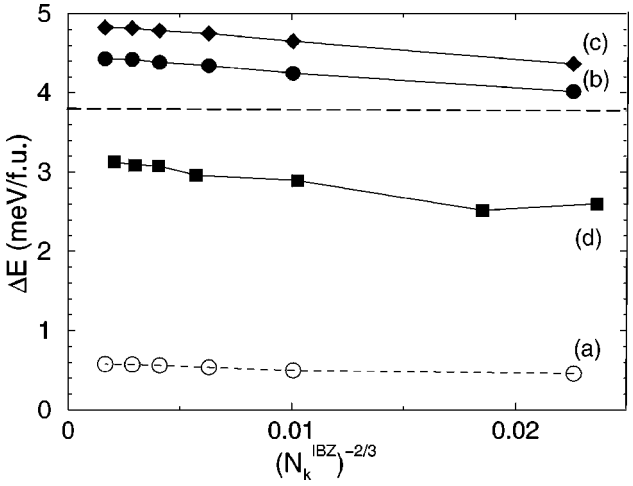

FIG. 2. Convergence of the MA energy of YCo_5 as a function of the number of **k** points in the irreducible part of the Brillouin zone used for the reciprocal-space integration in the present calculation. Four results are shown, corresponding to calculations (a) to (d) (see text). The experimental value is indicated by a horizontal dashed line.

the anisotropy of the magnetization mainly arises from the $2c$ site. This trend is confirmed by our calculation although the calculated OMA's of $0.02\mu_B$ and $0.05\mu_B$ for YCo_5 ($0.02\mu_B$ and $0.07\mu_B$ for $NdCo_5$) at the $3g$ and $2c$ site, respectively, are smaller than the magnetization anisotropies of $0.03\mu_B$ at the $3g$ site and $0.10\mu_B$ at the $2c$ site reported in Ref. 1. The OMA's given by the difference of the orbital moments obtained in two independent self-consistent relativistic calculations with quantization axis (0001) and $(\bar{1}\bar{2}10)$, respectively, including OP, as discussed in Sec. IVB below, are larger, amounting to $0.05\mu_B$ at the $3g$ site and $0.08\mu_B$ at the $2c$ site for YCo_5. These OMA's and the resulting magnetization anisotropy are closer to experiment than those obtained from the one-step procedure outlined in Sec. III. We attribute this to the fact that the force theorem is not valid for the orbital moments. Despite this underestimation of the OMA by the one-step procedure due to the large relative size of the OMA of the Co atoms in YCo_5 we include the OMAs obtained in this way in the following since they nevertheless provide a reasonable breakdown of the total OMA and thus information on the origin of the total MA energy.

B. Magnetocrystalline anisotropy energy of YCo_5

In Fig. 2 the calculated MA energies $\Delta E = E_{\bar{1}\bar{2}10} - E_{0001}$ are plotted versus $N_k^{-2/3}$, with N_k denoting the number of **k** points in the irreducible part of the BZ. The $N_k^{-2/3}$ scaling, which is evident from the figure, derives from the fact that for bands whose dispersion within a tetrahedron is quadratic in **k**, the linear tetrahedron method gives rise to an error in the single-particle eigenvalue sum which is proportional to $(\delta k)^2$, i.e., to $v^{2/3}$ with v being the volume of a single tetrahedron[5] which in turn is proportional to $1/N_k$. N_k ranges from 294 to 14850 in Fig. 2. As can be seen, the MA energies converge quite well as a function of N_k. The deviation from the fully converged value is below 2% with N_k

$=2002$ and shows approximately the expected linear behavior in the chosen representation. In Fig. 2, MA energies from calculations (a) and (b), as described above, are shown. In order to get an idea of how much the difference between the scalar-relativistic and the relativistic potential and the difference between the OP shifts calculated self-consistently with the magnetization parallel and perpendicular to the c axis, respectively, influence the MA energy, we performed two further calculations. There, the MA energy was determined from two one-step calculations with the magnetization along the (0001) and $(\bar{1}2\bar{1}0)$ direction, respectively, in the self-consistent scalar-relativistic potential and including OP shifts obtained from a separate self-consistent relativistic calculation with the magnetization (c) parallel to the c axis and (d) parallel to the $(\bar{1}2\bar{1}0)$ direction.

We arrive at anisotropy energies of 0.58 meV/f.u. with (a) 4.4 meV/f.u. with (b) 4.8 meV/f.u. with (c) and 3.2 meV/f.u. with (d). The easy axis is always along the c direction. This has to be compared with the experimental anisotropy of 3.8 meV/f.u. derived from magnetization measurements at 4.2 K.[1] Hence the MA energy is severely underestimated by calculation (a) taking only spin-orbit coupling into account. This is related to the underestimation of the orbital moments and their anisotropies in comparison with experiment in this case, as discussed in the previous subsection. The OP correction considerably improves the agreement of the calculated MA energy with experiment by enhancing the orbital moments and the OMA's, which also brings them closer to the experimental orbital moments and their anisotropies. Calculation (b) only slightly overestimates the MA energy in comparison with experiment. The difference between calculations (b) and (c) is relatively small. The MA energy calculated by method (d) deviates more from the result of calculation (b) because the self-consistently calculated orbital moments and hence also the OP shifts are considerably smaller when the magnetization is in $(\bar{1}2\bar{1}0)$ direction than when it is along the c axis—a consequence of the large OMA of the system.

In the following we will only refer to calculations of type (a) and (b). The calculated MA energy of 4.3 meV/f.u. between the $(10\bar{1}0)$ and (0001) direction, obtained by method (b), differs very little from that between $(\bar{1}2\bar{1}0)$ and (0001), i.e., the MA energy within the basal plane is negligible (≈ 0.1 meV/f.u.).

The MA energy ΔE, the OMA per unit cell ΔL and the OMA's ΔL_i of the two Co sites (multiplied with the number of equivalent sites per unit cell) of YCo_5 as a function of the band filling q are shown in Fig. 3. The band structures were calculated with the band filling (number of valence electrons) $q=48$ of YCo_5 using method (a) and method (b), respectively. Figure 3 is then obtained by varying the number of valence electrons (i.e., the position of the Fermi level) in the manner of a rigid-band model.

The shapes of ΔE, ΔL, and ΔL_i in Fig. 3 compare well with those reported in the literature.[3,43] However, we find the $2c$ site to contribute more to the total OMA at the Fermi level ($q=48$) than the $3g$ site, whereas the opposite was reported in Refs. 3 and 43. We attribute this to the larger

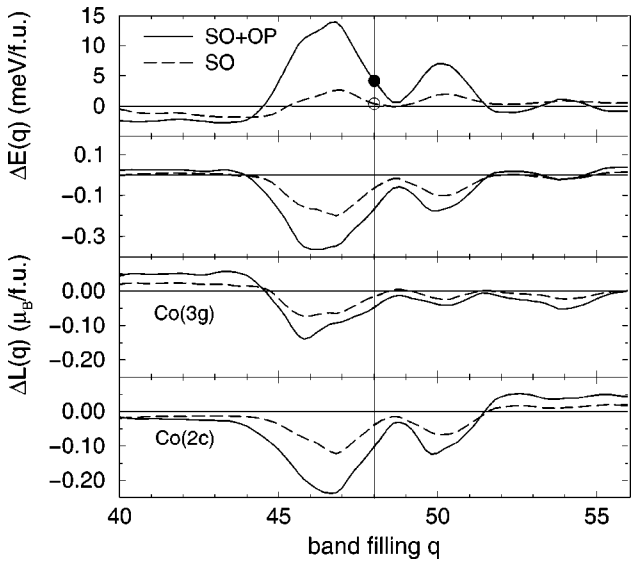

FIG. 3. MA energy ΔE and OMA ΔL of YCo_5 calculated including spin-orbit coupling only (dashed lines) and including both spin-orbit coupling and orbital polarization (solid lines), respectively, as a function of band filling q. The Fermi energy of YCo_5 corresponds to $q=48$, indicated by a vertical line. The contributions of the Co($3g$) and the Co($2c$) sites to the total OMA are given in the lower two panels.

orbital moment at the $2c$ site found in our calculation, cf. the previous subsection. The dependence of the MA energy and OMA on band filling has been extensively discussed by Daalderop *et al.*[3] In brief, the peak structure in Fig. 3 is related to the band structure in the vicinity of the Fermi level, to the lifting of band degeneracies at high-symmetry **k** points and along symmetry lines by SO splitting. Because of the anisotropy of hybridization in the hexagonal system YCo_5, the orbital moment and, hence, the SO splitting is different for different orientations of the magnetization, thus inducing a MA. The OP correction enhances the orbital moment and causes an additional OP splitting, amplifying the peaks in ΔE, but leaves the shape of the band-filling dependence almost unchanged. It is obvious from Fig. 3 that the T anisotropy of RT intermetallics (and other transition-metal systems with uniaxial crystal structure) could, at least in principle, be considerably larger than that of YCo_5 which is about 0.88 meV/Co atom in our calculation.

C. Dependence on c/a ratio

It is interesting to investigate how the itinerant-electron MA energy depends on the lattice geometry, e.g., on the c/a ratio of a uniaxial crystal, for several reasons.

(1) Nowadays, crystals with modified lattice geometries can be made by epitaxial growth on suitably chosen substrates, for example Fe with tetragonal structure.[51] RT compound films have been grown successfully, too.[52,53]

(2) It is often assumed that the T sublattice anisotropy of isostructural RT intermetallics with different rare earths is the same,[26] but the c/a ratios of isostructural RT compounds with different rare earths can vary considerably, cf. the values given for RCo_5 in Table II. In addition, the c/a ratio may

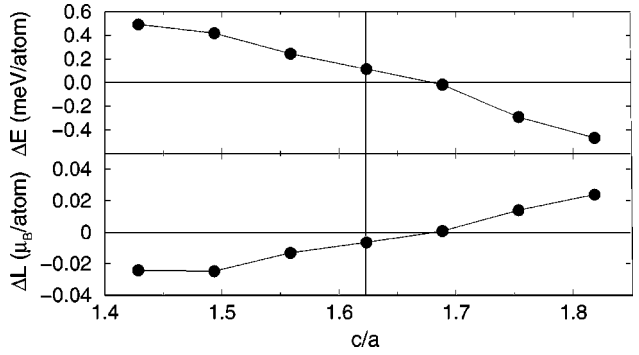

FIG. 4. MA energy ΔE and OMA ΔL of hcp Co as a function of the c/a ratio (orbital polarization correction included). The volume has been kept constant. The vertical line corresponds to the experimental value $c/a=1.6232$ for bulk hcp Co. The anisotropy changes from easy-axis to in-plane at $c/a\approx 1.688$.

change as a function of temperature or under pressure. These lattice geometry changes will alter the band structure and, thus, have an impact on the MA energy. An example for an experimentally established relation between the MA energy and the c/a ratio is the anomalous maximum in the temperature dependence of the MA energy of $Y_2Fe_{14}B$ which coincides with a maximum in the c/a ratio.[54]

(3) Szpunar and Lindgård[55] suggested a phenomenological single-ion-like model in which the MA energy of a uniaxial system is determined by the deviation of the c/a ratio from its ideal value $\sqrt{\frac{8}{3}}$ and changes its sign at this value. This simple picture may provide rough estimates of sign and order of magnitude of the anisotropy in simple cases but it is not likely to hold for more complex systems involving several sublattices and crystallographically nonequivalent sites. In our opinion, the changes of the MA energy in dependence on the c/a ratio are better described as being due to changes of the band structure as a function of the c/a ratio; see, e.g., Fig. 6 below.

We performed calculations of the MA energy and OMA of YCo_5 where the c/a ratio was varied (i) keeping the lattice parameter a constant and (ii) at constant volume.

Before addressing the more involved case of YCo_5, we briefly look at the c/a ratio dependence (at constant volume) of MA energy and OMA of hcp Co. The result, calculated including orbital polarization, is shown in Fig. 4, where ΔE and ΔL are plotted versus c/a. The calculated MA energy of 100 μeV/atom (favoring c-axis orientation of the magnetization) is in qualitative agreement with the value of 81 μeV/atom recently obtained from full-potential total-energy calculations[8] and fairly close to the experimental value of 65 μeV/atom.[56] The MA and OMA of hcp Co is found to change from easy-axis to in-plane at $c/a\approx 1.688$. The occurrence of this spin reorientation is in qualitative agreement with the phenomenological model of Szpunar and Lindgård,[55] although the change of sign occurs at a c/a value which is larger than $\sqrt{\frac{8}{3}}\approx 1.633$. The uniaxial MA energy and OMA are strongly enhanced when the c/a ratio is lowered.

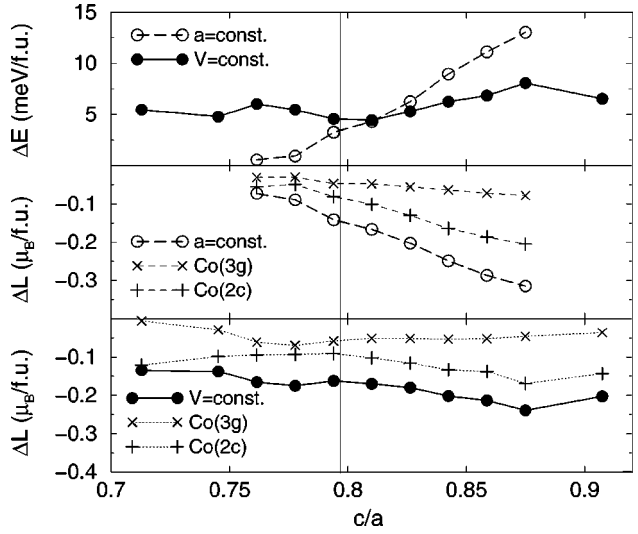

FIG. 5. MA energy ΔE and OMA ΔL of YCo_5 as a function of the c/a ratio, calculated (including orbital polarization) at (i) constant lattice parameter a (open circles) and (ii) constant volume (filled circles). The vertical line corresponds to the experimental value $c/a=0.8101$ for YCo_5. The respective OMA's of the two crystallographically inequivalent Co sites are also included in the lower two panels.

In YCo_5, the MA energy and OMA grows almost linearly with increasing c/a ratio if the lattice parameter a is kept constant, cf. Fig. 5 (open circles). The OMA contributions of the two Co sites exhibit a similar dependence on c/a, but the dependence is notably stronger for the $2c$ site. The change of the MA energy is, therefore, dominated by the $2c$ site. The enhancement of OMA and MA energy seems to be in line with the naive picture that increasing the lattice parameter c reduces the hybridization in c direction which—with the hybridization in the ab plane remaining constant—enhances the anisotropy of hybridization and thus the OMA. However, details of the band structure seem to be important, too, since, if the c/a ratio is varied at constant volume, the dependence of the MA energy and OMA on c/a is much weaker and less systematic, see Fig. 5 (filled circles). The easy axis remains parallel to the c direction at all calculated c/a ratios. The c/a dependence of the MA energy roughly mirrors that of the OMA although the two are not strictly proportional. The much weaker dependence of the OMA on the c/a ratio in this case is due to the different and partially compensating behavior of the two nonequivalent Co sites in this case. The $2c$ site anisotropy exhibits a maximum as a function of the c/a ratio, whereas the $3g$ site anisotropy goes through a minimum (note, that the site anisotropies have been multiplied with the number of equivalent sites per unit cell).

In a film geometry, the change of the c/a ratio due to the lattice mismatch between film and substrate is usually such that the volume of the bulk material is roughly conserved in the film. Hence, we expect a large uniaxial intrinsic contribution to the MA, similar to the bulk value, for a thick YCo_5 film.

In Fig. 6, the MA energy and OMA are plotted as a function of band filling q at various c/a ratios. The large peak in

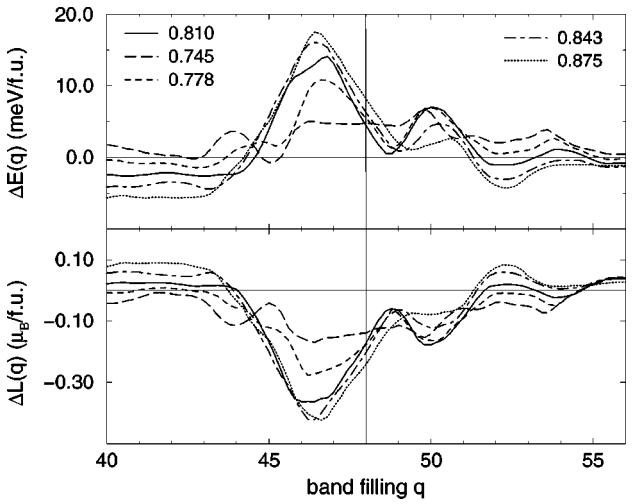

FIG. 6. Same as Fig. 3 for different values of the c/a ratio (volume kept constant, orbital polarization included).

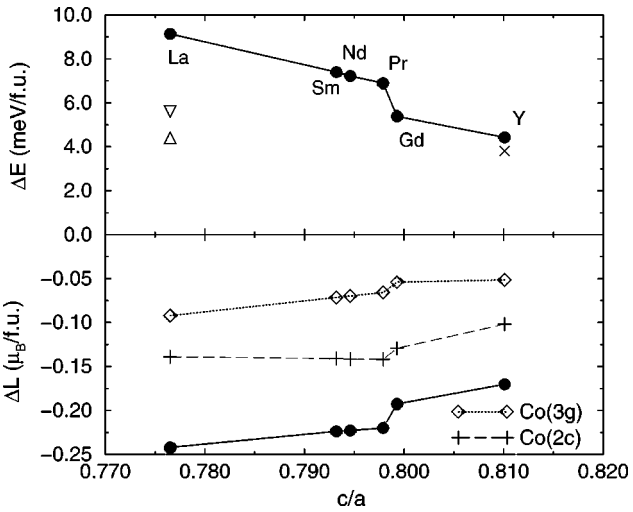

FIG. 7. MA energy ΔE, OMA ΔL and OMA contributions of the two crystallographically inequivalent Co sites of $R\mathrm{Co}_5$ (R = La, Nd, Sm, Pr, Gd, Y) calculated (including orbital polarization) at the experimental lattice parameters and plotted as a function of the c/a ratio (see text). Experimental values of the MA energy for YCo_5 ($\times$, Ref. 1) and LaCo_5 ($\triangle$, Ref. 57, and $\triangledown$, Ref. 2) are given for comparison.

$\Delta E(q)$ just below Fermi filling, and, consequently, also the MA energy given by the value at Fermi filling, is enhanced by increasing c/a, mainly due to an enhancement of the $2c$ site OMA. The $3g$ site OMA peak below the Fermi energy diminishes, but its contribution to the total anisotropy remains almost unchanged. Reducing the c/a ratio gradually destroys the large peak in $\Delta E(q)$. However, this does not significantly diminish the MA energy at Fermi filling.

D. $R\mathrm{Co}_5$ with other rare earths

The anisotropy contributions of the T and R sublattice in RT intermetallics with partially filled R $4f$ shell cannot be separated in magnetization measurements. Such a separation is only of limited significance anyway because of the interaction between the d and f electrons which results in a mutually induced polarization. This is particularly the case for the R $5d$ states which are polarized by the R $4f$ states and which contribute to the MA energy, too. We checked the influence of the polarization of the $4f$ shell on the calculated itinerant-electron MA energy of $R\mathrm{Co}_5$ and found it to be very small except for Gd where it decreases the MA energy by about 15%. Direct observation of $4f$ crystal-field excitations by inelastic neutron scattering provides independent information on the $4f$ anisotropy but such measurements are difficult and often impossible for ferromagnetic RT intermetallics. Therefore, it is usually assumed that the T sublattice anisotropy of a given RT compound is the same as that of the isostructural Y (La,Lu) compound. However, in many cases, the lattice geometry of RT systems varies considerably as a function of the rare earth. For example, the volume of $R\mathrm{Co}_5$ decreases and the c/a ratio changes significantly along the R series, as a consequence of the lanthanide contraction (see Table II). The smaller c/a ratio of LaCo_5 in comparison with YCo_5 can be easily understood in a rigid-sphere picture. The lattice is widened in the basal plane [containing R($1a$) and Co($2c$) atoms] in order to accommodate the larger La atoms. This enables the Co($3g$) atoms to move closer towards the R($1a$)-Co($2c$) plane and c decreases. These lattice-geometry changes can significantly influence band structure, OMA and MA energy.

We calculated the itinerant-electron MA energies of $R\mathrm{Co}_5$ (R=Y, La, Pr, Nd, Sm, Gd) at the experimental lattice geometries and find a surprisingly large variation of the MA energy, cf. upper panel of Fig. 7, along the R series. The dependence of the MA energy on the c/a ratio along the R series (shown in Fig. 7) is not smooth since the volume change appears to influence the MA energy significantly, too. The volumes of NdCo_5, SmCo_5, and PrCo_5 are very similar. GdCo_5 and YCo_5 have notably smaller volumes, while the volume of LaCo_5 is larger. In addition, as already mentioned, the influence of the $4f$ polarization is much stronger for GdCo_5 than for the other compounds. The OMA (lower panel of Fig. 7) diminishes by about 30% between LaCo_5 and YCo_5 while the orbital moment (not shown) is lowered by about 20%. This results in a strong variation of the MA energy between LaCo_5 and YCo_5. Experimentally, the T sublattice anisotropy can be directly measured only for the Y and La compound where the $4f$ shell is empty. In other $R\mathrm{Co}_5$ compounds, the $4f$ electrons provide a large part of the total anisotropy energy, either by their interaction with the crystal field or, in case of Gd, by dipolar interaction and anisotropic exchange. Anisotropy energies of 4.4 meV/f.u. and 5.6 meV/f.u. are obtained from the measured anisotropy constants K_1 (at 4.2 K) of LaCo_5 reported in Refs. 57 and 2, respectively. These MA energies are larger than the value of 3.8 meV/f.u. derived from the experimental K_1 and K_2 measured on YCo_5,[1] but the difference is smaller than that obtained in the calculation. The difference in the calculated MA energies for YCo_5 and LaCo_5 is predominantly due to the altered lattice geometry, since a calculation for LaCo_5 at the experimental lattice parameters of YCo_5 yields only a

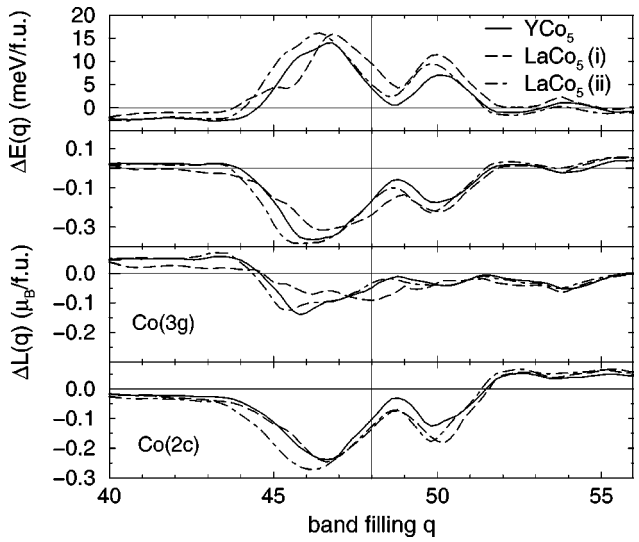

FIG. 8. Same as Fig. 3 for YCo_5 (solid lines) and $LaCo_5$ calculated at the experimental lattice geometries of (i) $LaCo_5$ (dashed lines) and (ii) YCo_5 (dot-dashed lines), including both spin-orbit coupling and orbital polarization.

slight increase (4.9 versus 4.4 meV/f.u.) of the MA energy in comparison with YCo_5. Including the (unoccupied) $4f$ states into the valence basis in $LaCo_5$ decreases the calculated MA energy only by about 10% and cannot remedy the discrepancy between theory and experiment. A dipolar MA energy of 0.05 meV/f.u. was calculated for YCo_5.[3] For a hcp lattice, the dipolar MA energy is proportional to the deviation of the c/a ratio from its ideal value, $\sqrt{\frac{8}{3}}$.[5] Under the assumption that the c/a ratio dependence in RCo_5 compounds is approximately of this kind, the dipolar MA energy in $LaCo_5$ would be about six times larger than in YCo_5—still much too small to explain the difference between calculated and experimental MA energy of $LaCo_5$.

In Fig. 8 the calculated MA energies and OMA's of RCo_5 (R=Y, La) are plotted as a function of band filling. It can be seen that the large variation of the MA energy at Fermi filling results from relatively small changes of height, width, and position of the small peak just (about 0.1 eV) below the Fermi level. Replacing Y by La in the YCo_5 lattice enhances and broadens this peak. When the change of the lattice geometry between YCo_5 and $LaCo_5$ is taken into account, the peak is shifted to higher energies. This strongly enhances the calculated MA energy. (The OMA of the $2c$ site which is in the basal R-Co plane increases slightly when Y is replaced by the larger La. The additional modification of the lattice geometry leaves the $2c$ site almost unchanged but causes a strong enhancement of the $3g$ site OMA which gives rise to the enhancement of the MA energy.)

E. Fe substitution

In this subsection we investigate how substitution of Co by Fe influences the MA energy and OMA. YFe_5 does not form but pseudobinaries $Y(Co_{1-x}Fe_x)_5$ have been made and their magnetic anisotropy has been measured,[58–60] although the experimental information is not as complete as for other pseudobinary systems such as $Y_2(Fe_{1-x}Co_x)_{17}$.[59–61] We calculated the MA energies and OMA's of YCo_5, hypothetical YFe_5 and the ordered pseudobinaries YFe_3Co_2 and YCo_3Fe_2. The experimental lattice parameters of YCo_5 were used for all these compounds in order to exclude lattice geometry effects. Experimental information on the lattice geometry is not available for the ordered pseudobinaries. Recently, the lattice parameters of the pseudobinary alloys $Y(Co_{1-x}Fe_x)_5$ were determined for $0 \leqslant x \leqslant 0.4$ and extrapolated to higher Fe concentrations.[62] Volume and c/a ratio were found to increase by about 4% and 1%, respectively, in the measured concentration range. Hence, we do not expect lattice geometry changes to be of major importance in the concentration range $0 \leqslant x \leqslant 0.26$ where experimental data on the MA exist.

In Table IV, the calculated spin and orbital moments and total magnetizations for magnetization directions (0001) and $(\bar{1}\bar{2}10)$ and the total OMA's ΔL and MA energies ΔE of ordered $Y(Co_{1-x}Fe_x)_5$ (x=0,0.4,0.6,1.0) are given. They

TABLE IV. Same as Table III for ordered $Y(Co_{1-x}Fe_x)_5$ (x=0,0.4,0.6,1.0) compounds [calculation (b); see text].

	YCo_5		YCo_3Fe_2		YFe_3Co_2		YFe_5	
	spin	orbital	spin	orbital	spin	orbital	spin	orbital
Y($1a$)	-0.18	-0.01	-0.13	-0.03	-0.12	-0.02	-0.12	-0.04
	0.013	-0.020	-0.002	-0.001	-0.018	-0.013	-0.017	0.007
T($3g$)	1.52	0.26	1.35	0.18	1.94	0.12	1.60	0.07
	-0.002	-0.020	-0.001	-0.006	0.002	0.004	0.000	0.006
T($2c$)	1.47	0.33	2.33	0.13	1.20	0.23	1.97	0.08
	-0.005	-0.053	0.001	-0.013	-0.002	-0.059	-0.002	0.002
Total	7.32	1.41	8.57	0.77	8.10	0.81	8.62	0.35
	-0.003	-0.186	-0.002	-0.041	-0.015	-0.105	-0.020	0.029
M	8.73		9.33		8.91		8.98	
	-0.189		-0.043		-0.120		0.009	
ΔE	4.4		-0.35		1.6		-0.91	

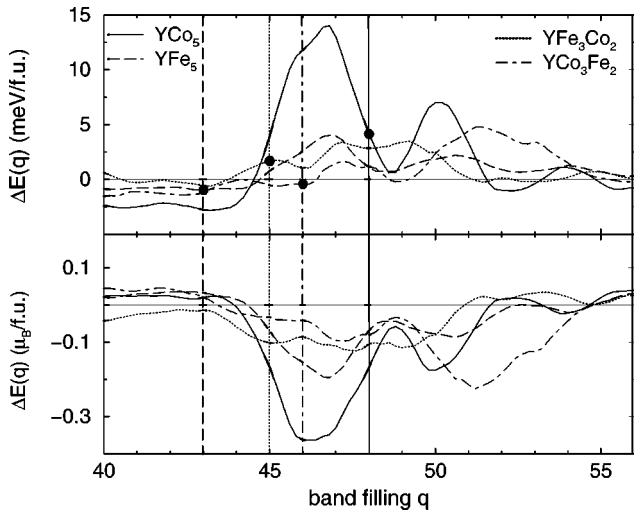

FIG. 9. Same as Fig. 3 for YCo_5 (solid line), YFe_5 (dashed line), YFe_3Co_2 (dotted line), and YCo_3Fe_2 (dot-dashed line). The Fermi energies of the respective compounds are indicated by perpendicular lines with corresponding line style.

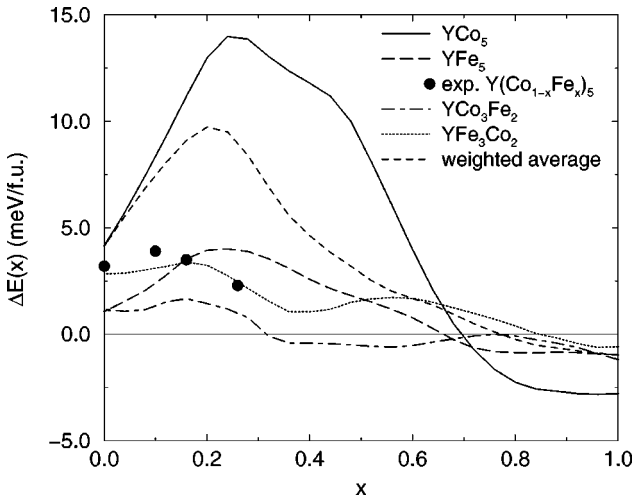

FIG. 10. Dependence of the MA energy of the pseudobinary compounds $Y(Co_{1-x}Fe_x)_5$ on the Fe concentration x as obtained from magnetization measurements (Refs. 58 and 60) (filled circles) in comparison with the band filling dependence of the calculated MA energy of YCo_5 (long-dashed line), YFe_5 (dashed line), YFe_3Co_2 (dotted line), and YCo_3Fe_2 (dot-dashed line). The band fillings q have been transformed into concentrations x by $q=48-5x$, i.e., by assuming a rigid-band behavior. The solid line is a weighted average, taking into account site preferences and the different SO parameter of Fe and Co (see text).

have been calculated including orbital polarization, corresponding to method (b) in Sec. IV B. Looking at the spin moments, we observe that the Fe moments are considerably larger in the pseudobinaries than in YFe_5. This is due to the presence of the Co atoms. The Fe spin moment increases with the number of Co neighbors, similar to the behavior of Fe in Fe-Co alloys.[63] The Fe orbital moments behave similarly but with larger relative changes. The Co spin and orbital moments diminish somewhat when Fe is substituted. The anisotropy of the spin moments is always very small.

In order to discuss the MA energies and OMA's, it is instructive to look at their dependence on band filling. This is shown in Fig. 9. The interplay of band structure, magnetization-direction dependent spin-orbit (and orbital polarization) splitting and band filling can be nicely seen in this figure. The shapes of $\Delta E(q)$ and $\Delta L(q)$ appear to be very similar for YCo_5 and YFe_5. $\Delta L(q)$ is proportional to the spin-orbit coupling parameter ξ which is about 50% larger for Co than for Fe. $\Delta E(q)$ scales like $(\frac{1}{2}\xi+BL)\Delta L$ (the anisotropy of spin and orbital-polarization splitting), is therefore roughly proportional to ξ^2 and increases much more between the Fe and the Co compound. The easy-axis anisotropy of the Co compound and the in-plane anisotropy of the Fe compound follows from the band-filling dependence of ΔE for both compounds. Hence, the change of anisotropy between YCo_5 and YFe_5 can be quantitatively explained by spin-orbit coupling strength and band filling if changes of the lattice geometry are excluded. $\Delta E(q)$ and $\Delta L(q)$ are much more altered (besides the effect of the lower spin-orbit parameter of Fe) when two different atom species are occupying the two T sites, reflecting a qualitative change of the band structure in the vicinity of the Fermi level, which is related to the change from the $CaCu_5$ to the $PrNi_2Al_3$ structure. The large peak in $\Delta E(q)$ at about $q=46.5$, which is mainly related to the lifting of a band degeneracy about 0.1 eV below E_F (of YCo_5) at the K point and has mainly Co($2c$) $d_{x^2-y^2}$ and d_{xy} character,[3] is strongly reduced in YFe_3Co_2 and YCo_3Fe_2, so the actual MA energies for these two compounds are much smaller than what would be expected from a simple band-filling argument.

The Fe concentration dependence of the MA constant K_1 of $Y(Co_{1-x}Fe_x)_5$ alloys has been measured[58] for $0\leqslant x\leqslant 0.26$ at room temperature and multiplied with the ratio of K_1 at 4.2 K and 300 K of YCo_5[1] in order to get the zero-temperature K_1.[59] The resulting experimental MA energies are given by the filled circles in Fig. 10. In a rigid-band model, the variation of the MA energy ΔE of $Y(Co_{1-x}Fe_x)_5$ alloys as a function of x follows immediately from its dependence on band filling: $\Delta E(x)=\Delta E(q=48-5x)$. Figure 10 exhibits the dependence of the calculated MA energy on the concentration x derived in this way for YCo_5, YFe_5, YFe_3Co_2, and YCo_3Fe_2. Neutron diffraction studies[64] revealed that the slightly larger Fe atoms preferentially occupy the $3g$ site while the smaller Co atoms prefer the $2c$ site in the isostructural $Th(Co_{1-x}Fe_x)_5$ series. Hence, it is likely that at low concentrations the Fe atoms are preferentially substituted at the $3g$ site in $Y(Co_{1-x}Fe_x)_5$, too. This could be simulated by taking the weighted averages $(1-x_{3g})\Delta E_{YCo_5}(x)+x_{3g}\Delta E_{YFe_3Co_2}(x)$ in $0\leqslant x\leqslant 0.6$ and $(1-x_{2c})\Delta E_{YFe_3Co_2}(x)+x_{2c}\Delta E_{YFe_5}(x)$ for $x>0.6$. All calculated band-filling dependences exhibit a maximum at an Fe concentration of about 20%, in qualitative agreement with experiment. However, the huge enhancement of the MA energy upon increasing the band filling calculated for YCo_5, which is transferred to the weighted average between YCo_5 and YFe_3Co_2 because of the large weight given to YCo_5 at low Fe concentrations, is not observed in experiment. Rather, the experimental values are close to the calculated curve for

YFe_3Co_2. This suggests that at low Fe concentrations the pseudobinary alloy adopts the $PrNi_2Al_3$ structure, with Fe and Co randomly distributed at the $3g$ sites and Co at the $2c$ sites. An alternative explanation would be that the large MA energy is reduced by disorder. Fully relativistic CPA calculations are necessary to resolve that matter. Finally, the experiments were carried out on polycrystalline samples,[58] yielding a 20% smaller MA energy for YCo_5 than the single-crystal measurements.[1]

The MA energies of YCo_5, YFe_5, and YFe_3Co_2 have been calculated by Trygg *et al.*[20] These authors find a small negative (in-plane) anisotropy for YFe_5 and a large positive (easy-axis) anisotropy for YFe_3Co_2, in agreement with the results of the present work.

F. Site decomposition of the anisotropy energy

So far, we discussed the MA energy in a reciprocal-space picture, based on band structure and band-filling arguments, in accordance with the itinerant character of the *d* states in the considered compounds. On the other hand, it would be desirable to complement this by a real-space (local) description, for example in order to analyze the origin of the MA energy in terms of contributions from different sites in the unit cell. The intimate relation between MA energy and OMA, which is a local, site-projected quantity, suggests that such a description should be possible. A decomposition of the MA energy into site contributions can be achieved in different ways.

(1) Within perturbation theory, the MA energy of a uniaxial system can be approximated by the sum of the differences of the OMAs for spin-up and spin-down states for each atom in the unit cell, weighted with the spin-orbit parameter of the atom, provided that the exchange splitting is large in comparison with the bandwidth:[65,66]

$$\Delta E \approx \sum_i \left[\frac{\xi_i}{4\mu_B} (\Delta L_i^+ - \Delta L_i^-) \right]. \tag{7}$$

By including orbital polarization, we generalize this to

$$\Delta E \approx \sum_i \left[\frac{1}{2\mu_B} \left(\frac{1}{2} \xi_i + B_i L_i \right) (\Delta L_i^+ - \Delta L_i^-) \right]. \tag{8}$$

Equation (8) provides a reasonable estimate of the site anisotropies. This is illustrated by Table V, which contains the calculated *d* orbital moments, spin-up and spin-down OMA's of the $Y(Co,Fe)_5$ compounds, and the site and total MA energies derived from these values by means of Eq. (8). However, the anisotropy contributions of equivalent sites in different compounds are, in general, completely different [compare, e.g., the Co($3g$) site anisotropies in YCo_5 and YCo_3Fe_2] because of the modification of the band structure. Hence, site decomposition does not provide any information which could be used to predict the MA energies of isostructural compounds.

(2) The MA energy is approximated by integrating over the difference of the site-projected integrated *d* DOS $N_i(\varepsilon,\hat{\mathbf{n}})$ for magnetization directions $\hat{\mathbf{n}}_1$ and $\hat{\mathbf{n}}_2$, respectively, to a common Fermi energy (for a derivation see, e.g., Ref. 14):

$$\Delta E \approx \sum_i \int^{\varepsilon_F^{(1)}} d\varepsilon [N_i(\varepsilon,\hat{\mathbf{n}}_2) - N_i(\varepsilon,\hat{\mathbf{n}}_1)]. \tag{9}$$

This procedure converges well with respect to the BZ integration and can be expected to provide a reasonable breakdown of the total MA energy into site contributions. It has been applied to derive the *d*-state site contributions to the MA energy of YCo_5 which are shown in Fig. 11 in dependence on band filling. The site decomposition, given by the site-projected integrated *d* DOS values at the Fermi level, is similar to that obtained from Eq. (8).

Attempts to decompose the MA energy of RT intermetallics into contributions of the different crystallographic sites have also been made from the experimental side.[23,59–61,67,68] Based on the assumption that the single-ion model is valid to some extent for the T sublattice anisotropy, site anisotropies have been derived from the concentration dependence of the MA constant $K_1(x)$ in $R_n(Co_{1-x}Fe_x)_m$ compounds.[59] The difference $\Delta K_1^i = K_{1,Fe}^i - K_{1,Co}^i$ of the Fe and Co site anisotropies has been determined by fitting the measured $K_1(x)$ to the following expression:

TABLE V. Orbital moments parallel and perpendicular to the hexagonal *c* axis and orbital moment anisotropies for spin-up and spin-down *d* states of Co, Fe, and Y in YCo_5, YCo_3Fe_2, YFe_3Co_2, and YFe_5 [calculation (b); see text]. In the last but one column the anisotropy energy contributions ΔE^{PT} of the *d* states of all equivalent sites of each kind are given which have been derived from the spin-up and spin-down orbital moment anisotropies by applying the perturbation-theory expression Eq. (8) (see text). For comparison, the anisotropy energies obtained from the full calculation are given in the last column.

	$\Delta L_{d,i}^{\uparrow}$ (μ_B)	$\Delta L_{d,i}^{\downarrow}$ (μ_B)	ΔE^{PT} (meV/f.u.)	ΔE (meV/f.u.)
YCo_5			5.1	4.4
Y($1a$)	-0.011	-0.006	-0.05	
Co($3g$)	-0.001	-0.017	2.0	
Co($2c$)	-0.006	-0.047	3.2	
YCo_3Fe_2			-0.1	-0.35
Y($1a$)	-0.012	0.010	-0.2	
Co($3g$)	-0.003	-0.002	-0.1	
Fe($2c$)	-0.004	-0.010	0.2	
YFe_3Co_2			2.5	1.6
Y($1a$)	-0.008	-0.010	0.02	
Fe($3g$)	-0.001	0.004	-0.3	
Co($2c$)	-0.007	-0.049	2.8	
YFe_5			-0.8	-0.91
Y($1a$)	-0.008	0.010	-0.2	
Fe($3g$)	0.001	0.005	-0.2	
Fe($2c$)	-0.005	0.006	-0.4	

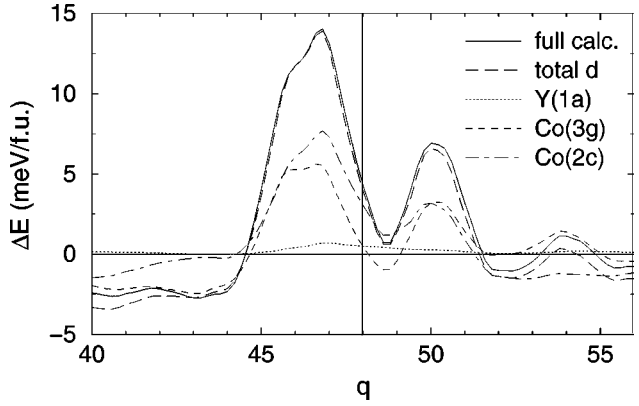

FIG. 11. Site decomposition of *d*-state contribution to the MA energy of YCo_5 [method (b)] as obtained from Eq. (9) plotted as a function of band filling.

$$K_1(x) = K_1(0) + \sum_i n_i f_{i,\mathrm{Fe}}(x) \Delta K_1^i, \tag{10}$$

where i is the crystallographic site, n_i the number of equivalent sites in the unit cell and $f_{i,\mathrm{Fe}}(x)$ the relative occupancy of site i by Fe atoms which is obtained from neutron diffraction. $K^i_{1,\mathrm{Fe}}$ can be deduced if $K^i_{1,\mathrm{Co}}$ is known from other experiments or vice versa. $K^i_{1,\mathrm{Co}}$ and $K^i_{1,\mathrm{Fe}}$ can indirectly be determined from the anisotropy of the hyperfine field obtained in nuclear magnetic resonance (NMR) and Mössbauer measurements, respectively.[59] The results of this procedure are based on the assumption that the local anisotropies of Fe and Co on each site are independent of x, i.e., that the charge distributions of Fe and Co are the same for a given site. Often, contributions of different signs for different sites are obtained from Eq. (10), in many cases leading to implausibly large site anisotropies compensating each other. The site anisotropies are sometimes also contradicting the results of other experiments. Fitting the measured $K_1(x)$ of $Y(Co_{1-x}Fe_x)_5$ (Ref. 58) by means of Eq. (10),[60] using site occupancies reported in Ref. 64, yields different signs for ΔK_1^i for the $3g$ and the $2c$ site. Then, Co site anisotropies $K^i_{1,\mathrm{Co}}$ deduced from NMR experiments[23] are used to derive $K^i_{1,\mathrm{Fe}}$. However, these Co site anisotropies are negative for the $3g$ site and positive for the $2c$ site, whereas the magnetization anisotropy deduced from polarized neutron diffraction on $NdCo_5$ (Ref. 1) is positive for both Co sites. Moreover, the sum of the Co site OMA's derived from NMR (Ref. 23) is much smaller than the measured[1] magnetization anisotropy of YCo_5.[69] No correspondence between the site anisotropies obtained from the fit, Eq. (10),[59] and the site anisotropies derived theoretically by means of Eq. (8) or (9) can be established. Pirogov *et al.*[67,2] derived site anisotropies corresponding to 2 meV/f.u. and 1.6 meV/f.u. for the $2c$ and $3g$ site of YCo_5, respectively, using Eq. (10) and assuming $K^i_{1,\mathrm{Ni}} = 0$, which provide a better fit of the measured $K_1(x)$ in $Y(Co_xNi_{1-x})_5$ pseudobinaries than those of Ref. 23 and are consistent with the theoretical values obtained in the present work. Nevertheless, bearing in mind the marked dependence of the MA energy on band filling and band structure, which in turn may be strongly influenced by lattice geometry changes, we conclude that the assumed independence of the site anisotropy on the concentration is questionable since, in general, all these quantities will change in dependence on the concentration. Therefore, the site anisotropies derived for a particular compound do not allow to predict the MA energies of isostructural compounds.

V. CONCLUSIONS

We determined the spin and orbital moments, magnetizations, and itinerant-state MA energies of RCo_5 (R=Y, La, Pr, Nd, Sm, Gd) and ordered $Y(Co_{1-x}Fe_x)_5$ (x =0.4,0.6,1.0) compounds by means of fully relativistic density-functional calculations. Taking into account orbital polarization corrections enhances the calculated magnetization, magnetization anisotropy, orbital moments, OMA's and MA energy of YCo_5, leading to good agreement with available experimental data. In accordance with neutron-diffraction results, we obtain a larger orbital moment and OMA at the $2c$ site. Our MA energy calculations for uniaxially strained YCo_5 and for RCo_5 compounds show that variation of the lattice geometry (c/a ratio and volume) induces slight changes of the band structure, which can strongly affect the MA energy because of the pronounced band-structure dependence of the latter. This gives rise to a large variation of the calculated MA energy of RCo_5 along the R series, in contrast to the commonly assumed independence of the Co sublattice MA on the R constituent and to the reported experimental MA energy of $LaCo_5$. The uniaxial MA energy of YCo_5 is found to enhance strongly with increasing c/a ratio if the latter is varied at constant lattice parameter a, whereas the changes are much smaller if the c/a ratio is varied at constant volume. The band-filling dependence of the calculated MA energies of all considered $Y(Co_{1-x}Fe_x)_5$ (x=0,0.4,0.6,1.0) compounds exhibits a maximum at fillings corresponding to about $x=0.2$, in accordance with the experimentally observed trend in $Y(Co_{1-x}Fe_x)_5$ pseudobinaries. A site decomposition of transition-metal MA energies is doubtful since the changes of the band structure upon substitution do not allow to transfer the site MA energies obtained for one particular compound to another isostructural system. Future investigations should include both technical refinements (MA energy from full-potential total energy calculations instead of employing the force theorem; realistic simulation of disorder in case of the pseudobinary alloys) and improvements of the underlying density-functional scheme, particularly regarding the treatment of orbital polarization effects.

ACKNOWLEDGMENTS

This work was supported by the German Bundesministerium für Bildung und Forschung, project 13N7443. We thank K. Koepernik for performing FPLO calculations and K.-H. Müller and M. Wolf for stimulating and helpful discussions.

*Email address: L.Steinbeck@ifw-dresden.de

[1] J. M. Alameda, J. M. Givord, and Q. Lu, J. Appl. Phys. **52**, 2079 (1981).

[2] H. R. Kirchmayr and E. Burzo, in *Landolt-Börnstein Numerical Data and Functional Relationships in Science and Technology, New Series, Group III*, edited by H. P. J. Wijn (Springer, Berlin, 1990), Vol. 19d2.

[3] G. H. O. Daalderop, P. J. Kelly, and M. F. J. Schuurmans, Phys. Rev. B **53**, 14 415 (1996).

[4] H. J. F. Jansen, Phys. Rev. B **38**, 8022 (1988).

[5] G. H. O. Daalderop, P. J. Kelly, and M. F. H. Schuurmans, Phys. Rev. B **41**, 11 919 (1990).

[6] J. Trygg, B. Johansson, O. Eriksson, and J. M. Wills, Phys. Rev. Lett. **75**, 2871 (1995).

[7] O. Hjortstam, K. Baberschke, J. M. Wills, B. Johansson, and O. Eriksson, Phys. Rev. B **55**, 15 026 (1997).

[8] P. James, O. Hjortstam, L. Nordström, B. Johansson, J. M. Wills, and O. Eriksson (unpublished); P. James, Ph.D. thesis, Uppsala University, Uppsala, 1999.

[9] Y. Guo, W. Temmerman, and H. Ebert, J. Phys.: Condens. Matter **3**, 8205 (1991).

[10] D.-S. Wang, R. Wu, and A. J. Freeman, Phys. Rev. Lett. **70**, 869 (1993).

[11] G. H. O. Daalderop, P. J. Kelly, and M. F. J. Schuurmans, Phys. Rev. B **50**, 9989 (1994).

[12] G. H. O. Daalderop, P. J. Kelly, and M. F. J. Schuurmans, Phys. Rev. B **44**, 12 054 (1991).

[13] I. V. Solovyev, P. H. Dederichs, and I. Mertig, Phys. Rev. B **52**, 13 419 (1995).

[14] S. S. A. Razee, J. B. Staunton, and F. J. Pinski, Phys. Rev. B **56**, 8082 (1997).

[15] P. M. Oppeneer, J. Magn. Magn. Mater. **188**, 275 (1998).

[16] M. S. S. Brooks, B. Johansson, O. Eriksson, and H. Skriver, Physica B **144**, 1 (1986).

[17] R. Coehoorn and G. H. O. Daalderop, J. Magn. Magn. Mater. **104-107**, 1081 (1992).

[18] L. Nordström, M. S. S. Brooks, and B. Johansson, J. Phys.: Condens. Matter **4**, 3261 (1992).

[19] M. Yamaguchi and S. Asano, J. Appl. Phys. **79**, 5952 (1996).

[20] J. Trygg, L. Nordström, and B. Johansson, in *Physics of Transition Metals*, edited by P. M. Oppeneer and J. Kübler (World Scientific, Singapore, 1993), pp. 745–748.

[21] A. Sakuma, J. Appl. Phys. **73**, 6922 (1993).

[22] A. Heidemann, D. Richter, and K. H. J. Buschow, Z. Phys. B **22**, 367 (1975).

[23] R. L. Streever, Phys. Rev. B **19**, 2704 (1979).

[24] J. Schweizer and F. Tasset, J. Phys. F: Met. Phys. **10**, 2799 (1980).

[25] M. Forker, A. Julius, M. Schulte, and D. Best, Phys. Rev. B **57**, 11 565 (1998).

[26] Apart from a rescaling of the temperature dependence of the anisotropy constants in order to take the changed Curie temperature into account.

[27] K. Buschow, Rep. Prog. Phys. **54**, 1123 (1991).

[28] J. J. M. Franse and R. J. Radwański, in *Handbook of Magnetic Materials*, edited by K. H. J. Buschow (Elsevier, Amsterdam, 1993), Vol. 7, pp. 307–501.

[29] M. Richter, J. Phys. D **31**, 1017 (1998).

[30] M. Brooks, O. Eriksson, and B. Johansson, J. Phys.: Condens. Matter **1**, 5861 (1989).

[31] J. Colpa, J. Magn. Magn. Mater. **104-107**, 1211 (1992).

[32] K. W. H. Stevens, Proc. Phys. Soc., London, Sect. A **65**, 209 (1952).

[33] M. T. Hutchings, Solid State Phys. **16**, 227 (1964).

[34] H.-S. Li and J. M. D. Coey, in *Handbook of Magnetic Materials*, edited by K. H. J. Buschow (North-Holland, Amsterdam, 1991), Vol. 6, pp. 1–83.

[35] D. Gignoux and D. Schmitt, in *Handbook on the Physics and Chemistry of Rare Earths*, edited by K. A. Gschneidner and L. Eyring (Elsevier, Amsterdam, 1995), Vol. 20, pp. 293-424.

[36] O. Eriksson, M. S. S. Brooks, and B. Johansson, Phys. Rev. B **41**, 7311 (1990).

[37] O. Eriksson, B. Johansson, R. C. Albers, A. M. Boring, and M. S. S. Brooks, Phys. Rev. B **42**, 2707 (1990).

[38] B. Johansson, O. Eriksson, L. Nordström, L. Severin, and M. S. S. Brooks, Physica B **172**, 101 (1991).

[39] J. P. Perdew and A. Zunger, Phys. Rev. B **23**, 5048 (1981).

[40] D. M. Ceperley and B. J. Alder, Phys. Rev. Lett. **45**, 566 (1980).

[41] H. Eschrig, *Optimized LCAO Method and the Electronic Structure of Extended Systems* (Springer-Verlag, Berlin, 1989).

[42] M. Richter and H. Eschrig, Solid State Commun. **72**, 263 (1989).

[43] M. Yamaguchi and S. Asano, J. Magn. Magn. Mater. **168**, 161 (1997).

[44] K. Koepernik and H. Eschrig, Phys. Rev. B **59**, 1743 (1999).

[45] M. Weinert, R. E. Watson, and J. W. Davenport, Phys. Rev. B **32**, 2115 (1985).

[46] P. James, O. Eriksson, B. Johansson, and L. Nordström (unpublished); P. James, Ph.D. thesis, Uppsala University, Uppsala, 1999.

[47] X. Wang, D.-S. Wang, R. Wu, and A. J. Freeman, J. Magn. Magn. Mater. **159**, 337 (1996).

[48] K. H. J. Buschow, Rep. Prog. Phys. **40**, 1179 (1977).

[49] A. V. Andreev, in *Handbook of Magnetic Materials*, edited by K. H. J. Buschow (Elsevier, Amsterdam, 1995), Vol. 8, pp. 59–187.

[50] O. Moze, L. Pareti, A. Paoluzi, and K. H. J. Buschow, Phys. Rev. B **53**, 11 550 (1996).

[51] J. Thomassen, F. May, B. Feldmann, M. Wuttig, and H. Ibach, Phys. Rev. Lett. **69**, 3831 (1992).

[52] E. E. Fullerton, C. H. Sowers, J. E. Pearson, S. D. Bader, J. B. Patel, X. Z. Wu, and D. Lederman, J. Appl. Phys. **81**, 5637 (1997).

[53] D. J. Keavney, E. E. Fullerton, Dongqui Li, C. H. Sowers, S. D. Bader, K. Goodman, J. G. Tobin, and R. Carr, Phys. Rev. B **57**, 5291 (1998).

[54] R. J. Radwański and J. J. M. Franse, in *Physics of Transition Metals*, edited by P. M. Oppeneer and J. Kübler (World Scientific, Singapore, 1993), pp. 782-785.

[55] B. Szpunar and P. A. Lindgård, J. Phys. F: Met. Phys. **9**, L55 (1979).

[56] D. Bonnenberg, K. A. Hempel, and H. P. J. Wijn, in *Landolt-Börnstein Numerical Data and Functional Relationships in Science and Technology, New Series, Group III*, edited by H. P. J. Wijn (Springer, Berlin, 1986), Vol. 19a.

[57] M. I. Bartashevich, T. Goto, M. Yamaguchi, and I. Yamamoto, J. Alloys Compd. **219**, 25 (1995).

[58] F. Rothwarf, H. A. Leupold, J. Greedan, W. E. Wallace, and D.

K. Das, Int. J. Magn. **4**, 267 (1973).
[59] J. J. M. Franse, N. P. Thuy, and N. M. Hong, J. Magn. Magn. Mater. **72**, 361 (1988).
[60] N. P. Thuy, J. J. M. Franse, N. M. Hong, and T. D. Hien, J. Phys. (Paris), Colloq. **49**, C8 (1988).
[61] N. P. Thuy and J. J. M. Franse, J. Magn. Magn. Mater. **54-57**, 915 (1986).
[62] F. Maruyama, H. Nagai, Y. Amako, H. Yoshie, and K. Adachi, Physica B **266**, 356 (1999).
[63] R. Richter and H. Eschrig, Phys. Scr. **37**, 948 (1988).
[64] J. Laforest and J. S. Shah, IEEE Trans. Magn. **MAG9**, 217 (1973).
[65] P. Bruno, Phys. Rev. B **39**, 865 (1989).
[66] P. James, O. Eriksson, and L. Nordström (unpublished); P. James, Ph.D. thesis, Uppsala University, Uppsala, 1999.
[67] A. N. Pirogov, A. S. Ermolenko, V. V. Kelarev, and S. K. Sidorov, Fiz. Met. Metalloved. **62**, 1035 (1986).
[68] Z.-H. Cheng, B.-G. Shen, F.-W. Wang, and H. Kronmüller, Appl. Phys. Lett. **74**, 1320 (1999).
[69] Part of the inconsistencies between the experimental results may be due to nonstoichiometry effects with additional Co statistically located at the *R* site in form of dumbbell pairs, a rather common situation in RCo_5 compounds (Refs. 2 and 24).